0013-7227/08/$15.00/0
Printed in U.S.A.

Endocrinology 149(10):4768–4777

doi: 10.1210/en.2008-0180

Brain Glucagon-Like Peptide 1 Signaling Controls the Onset of High-Fat Diet-Induced Insulin Resistance and Reduces Energy Expenditure

Claude Knauf,* Patrice D. Cani,* Afifa Ait-Belgnaoui, Alexandre Benani, Cédric Dray, Cendrine Cabou, André Colom, Marc Uldry, Sophie Rastrelli, Eric Sabatier, Natacha Godet, Aurélie Waget, Luc Pénicaud, Philippe Valet, and Rémy Burcelin

Institut de Medecine Moleculaire de Rangueil (I2MR) (C.K., P.D.C., C.D.,C.C., A.C., S.R., E.S., N.G., A.W., P.V., R.B.), Institut National de la Santé et de la Recherche Médicale Unité 858, Institut Fédératif de Recherche 31, Toulouse III University, Centre Hospitalier Universitaire Rangueil, 31432 Toulouse, France; Unit of Pharmacokinetics, Metabolism, Nutrition, and Toxicology (P.D.C.), Université Catholique de Louvain, 1200 Brussels, Belgium; Neuro-Gastroenterology and Nutrition Unit (A.A.-B.), Unité Mixte de Recherche 1054 Institut National de la Recherche Agronomique/ESAP, 31931 Toulouse, France; Laboratoire Métabolisme Plasticité Mitochondrie (A.B., L.P.), Toulouse III University, Centre National de la Recherche Scientifique Unité Mixte de Recherche 5241, 31432 Toulouse, France; and Dana-Farber Cancer Institute and Department of Cell Biology (M.U.), Harvard Medical School, Boston, Massachusetts 02115

Glucagon-like peptide-1 (GLP-1) is a peptide released by the intestine and the brain. We previously demonstrated that brain GLP-1 increases glucose-dependent hyperinsulinemia and insulin resistance. These two features are major characteristics of the onset of type 2 diabetes. Therefore, we investigated whether blocking brain GLP-1 signaling would prevent high-fat diet (HFD)-induced diabetes in the mouse. Our data show that a 1-month chronic blockage of brain GLP-1 signaling by exendin-9 (Ex9), totally prevented hyperinsulinemia and insulin resistance in HFD mice. Furthermore, food intake was dramatically increased, but body weight gain was unchanged, showing that brain GLP-1 controlled energy expenditure. Thermogenesis, glucose utilization, oxygen consumption, carbon dioxide production, muscle glycolytic respiratory index, UCP2 expression in muscle, and basal ambulatory activity were all increased by the exendin-9 treatment. Thus, we have demonstrated that in response to a HFD, brain GLP-1 signaling induces hyperinsulinemia and insulin resistance and decreases energy expenditure by reducing metabolic thermogenesis and ambulatory activity. (*Endocrinology* 149: 4768–4777, 2008)

THE INCIDENCE OF type 2 diabetes is increasing in Western countries and is now considered as an epidemic. Nowadays, it affects 150 million people and is treated with therapeutic strategies involving insulin secretion and/or action. Enteroendocrine cells have important roles in regulating energy intake and glucose homeostasis through their actions on peripheral target organs, including the endocrine pancreas. The incretin hormones, glucose-dependent insulinotropic polypeptide and glucagon-like peptide-1 (GLP-1), increase insulin secretion only in the presence of hyperglycemia and, consequently, glucose utilization in insulin-sensitive tissues (1). Of these two incretins, only GLP-1 has so far been considered for the development of therapeutic strategies, because unlike glucose-dependent insulinotropic polypeptide, it retains its insulinotropic effect in diabetic patients (2). GLP-1, which is released by the enteroendocrine L cells, is now considered as a leading hormone regulating glucose homeostasis in the absorptive state. In addition, GLP-1 is also released into the brain where it controls food intake and cardiovascular functions. Whereas most of the antidiabetic benefit has been attributed to the direct effect of the hormone on the pancreas, *i.e.* on glucose-stimulated insulin secretion, we and others have demonstrated important extra-pancreatic functions implicated in the control of glucose homeostasis. A recent observation was that mice lacking receptors for both incretins exhibited increased energy expenditure on normal chow (NC) as well as on high-fat diet (HFD) during both the light and dark phases of the feeding cycle (3). In the hepatoportal vein, the GLP-1 receptor is part of the portal glucose sensor mechanism (4) along with well-described molecules such as the glucose transporter GLUT2 (5, 6). In the presence of a positive portal to arterial glucose gradient, the glucose sensor sends a signal to the brain that dispatches the nutritional signals toward peripheral tissues and that increases muscle glucose utilization within minutes (7–9). Because the brain is now considered as a major center for the control of whole-body glucose homeostasis (10) we have previously shown that brain GLP-1 signaling is essential to stimulate insulin secretion in response to oral glucose. The infusion into the brain of the specific GLP-1 receptor antagonist exendin 9 (Ex9) inhibited the induction of insulin secretion by gut glucose (11). Our

First Published Online June 12, 2008
See editorial p. 4765.

* C.K. and P.D.C. have equally contributed.

Abbreviations: AMPK, AMP-activated kinase; BAT, brown adipose tissue; 2DG, 2-deoxyglucose; DIRKO, double incretin receptor knockout; eNOS, endothelial nitric oxide synthase; Ex9, exendin-9; GLP-1, glucagon-like peptide 1; HFD, high-fat diet; icv, intracerebroventricular; NC, normal chow; NEFA, nonesterified fatty acids; UCP1, uncoupled protein 1; WAT, white adipose tissue.

***Endocrinology* is published monthly by The Endocrine Society (http://www.endo-society.org), the foremost professional society serving the endocrine community.**

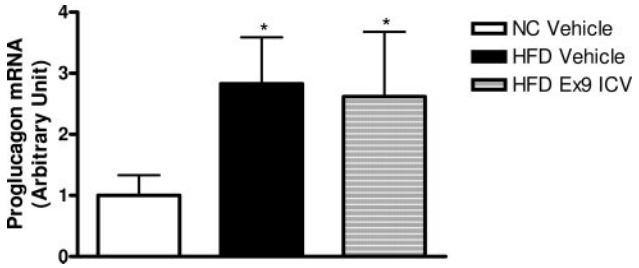

FIG. 1. HFD increases proglucagon mRNA concentration in the brainstem. Brainstem proglucagon mRNA concentration in mice fed a NC diet (NC Vehicle, n = 6) or a (HFD Vehicle, n = 6) and in Ex9 icv-treated mice fed a HFD (HFD Ex9 ICV, n = 7) for 2 wk. *, $P < 0.05$ *vs.* NC vehicle.

data suggested that the absorptive state was associated with the stimulation of the gut-to-brain axis leading to the activation of brain GLP-1 signaling and consequently to hyperinsulinemia. A further important discovery was that brain GLP-1 signaling induced insulin resistance by a mechanism that did not involve the muscle insulin receptor. The pathological consequence could be that an excessive stimulation of the gut-to-brain axis could lead to an overt activation of brain GLP-1 signaling. To test this hypothesis, we have determined the effect of a 1-month chronic blockage of brain GLP-1 on glucose homeostasis in HFD-fed mice. Ex9 was continuously infused into the lateral ventricle of the brain by means of a sc osmotic mini-pump. This procedure totally reversed both the insulin resistance and hyperinsulinemia induced by a HFD. This phenotype was further associated with the maintenance of normal body weight despite a considerably increased food intake. This could be explained by the observation that the blockage of brain GLP-1 increased energy expenditure through a mechanism involving metabolic thermogenesis. In conclusion, we have shown that the blockage of brain GLP-1 signaling prevents hyperinsulinemia and insulin resistance and favors energy expenditure when applied during the induction of diabetes by a HFD in mice.

Materials and Methods

Animals

Twelve-week-old C57BL6/J (Janvier, Saint Berthevin, France) male mice were housed with inverted 12-h daylight cycle (lights off at 1000 h). All the following animal experimental procedures have been validated by the local ethical committee of the Rangueil hospital. Mice were fed a NC (A04; Villemoisson sur Orge, France) or a high-fat, carbohydrate-free diet (HFD) for a period of 4 wk. The diet contained 72% fat (corn oil and lard), 28% protein, and less than 1% carbohydrate as energy content. This diet induces diabetes before the onset of obesity (12). Mice were separated into three groups: NC, HFD, and HFD treated with intracerebroventricular (icv) Ex9.

Surgical procedures

For all the surgical procedures, mice were anesthetized with isoflurane (Abbott, Rungis, France). An indwelling icv catheter was installed (13) and connected to an osmotic pump (Model 2004, Alzet; Cupertino, CA) delivering over 4 wk, at a rate of 0.25 μl/h, either artificial cerebrospinal fluid or Ex9 at a rate of 0.5 pmol/kg·min. This procedure allowed the catheter to be secured in place for the entire experimental period. Then, for the set of mice where iv infusion was to be carried out, 3 wk later, a catheter was installed into the femoral vein as previously described in detail (14). In a subset of mice, the osmotic pump was delivering Ex9 sc. These mice were used as control for the central role of Ex9.

Intraperitoneal glucose tolerance test

An ip glucose tolerance test was performed 3 wk after the beginning of the treatment as previously described (15).

Insulin sensitivity

Insulin sensitivity was assessed by the euglycemic hyperinsulinemic clamp as previously described (15) at completion of the treatment period, *i.e.* the fourth week. Briefly, 6-h-fasted mice were infused with insulin at a rate of 4 mU/kg·min (physiological) for 3 h, and D-[^{3}H]3-glucose (PerkinElmer, Boston, MA) was infused at rate of 30 μCi/kg·min to ensure a detectable plasma D-[^{3}H]3-glucose enrichment. Plasma glucose concentrations and D-[^{3}H]3-glucose-specific activity were determined in 5 μl blood sampled from the tip of the tail as previously described (16).

Glucose utilization by different tissues

To determine an index of the glucose utilization rate by different tissues, a rapid iv injection of 30μCi per mouse of D-[^{3}H]2-deoxyglucose (D-[^{3}H]2DG; PerkinElmer) was given through the femoral vein 60 min

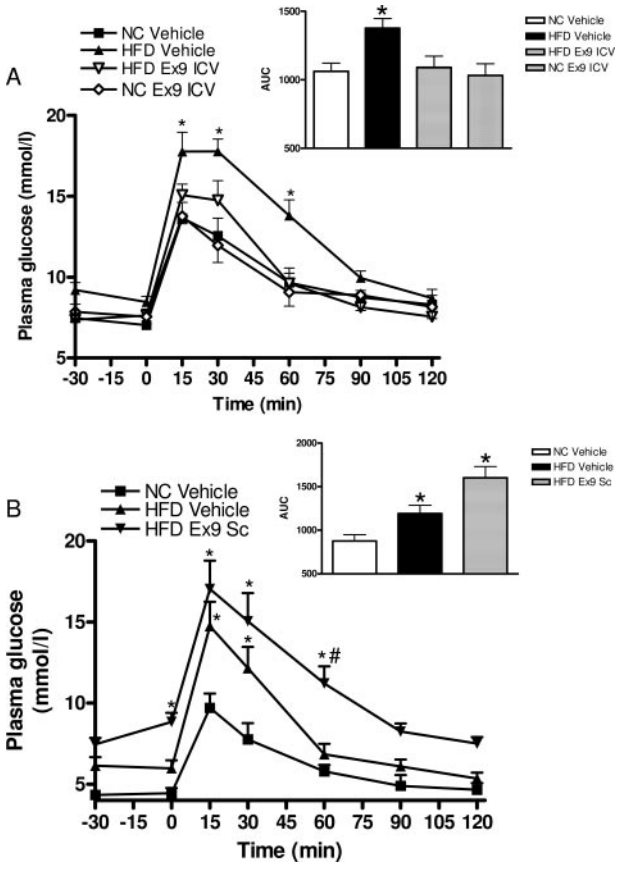

FIG. 2. Brain Ex9 treatment ameliorates glucose tolerance in HFD mice. Plasma glucose (millimoles per liter) after an ip glucose load (1 g/kg) in NC-fed mice fed and treated (NC Ex9 ICV n = 6) or not (NC Vehicle, n = 9) with Ex9 icv and in HFD-fed mice treated (HFD Ex9 ICV, n = 10) or not (HFD Vehicle, n = 9) with Ex9 icv (A). The *inset* represents the area under curve (arbitrary units) of the same groups. *, $P < 0.05$ *vs.* HFD Vehicle. Similar groups were studied in B with sc vehicle or Ex9 (NC Vehicle, n = 6; HFD Vehicle, n = 7; HFD Ex9 Sc, n = 11) for 4 wk. The *inset* represents the area under curve (arbitrary units) of the same groups. *, $P < 0.05$ *vs.* NC vehicle; #, $P < 0.05$ *vs.* HFD vehicle.

TABLE 1. Plasma parameters during fed state

Blood glucose (mmol/liter)				Insulinemia (μU/ml)			
NC	NCEx9	HFD	HFD/Ex9	NC	NC/Ex9	HFD	HFD/Ex9
8.83 ± 0.13	9.37 ± 0.44	9.07 ± 0.32	8.22 ± 0.16	23.51 ± 6.78	21.31 ± 2.23	49.87 ± 4.99[a]	29.95 ± 8.91

Plasma glucose and insulin concentrations in mice fed a NC diet.
(n = 9) or a HFD (n = 10) and in Ex9 icv-treated mice fed a NC (NC/Ex9, n = 6) or HFD (HFD/Ex9, n = 11) for 4 wk.
[a] $P < 0.05$ *vs.* all other groups.

before the end of the infusion period (16). Heart, vastus lateralis, brown adipose tissue (BAT), and white adipose tissue (WAT, corresponding to sc adipose tissue) were dissected out and immediately dissolved in NaOH to extract the D-[^{3}H]2DG-6-phosphate, as previously described (7).

Biochemical analyses

Glycemia and the plasma insulin concentrations were determined at the end of wk 4 in the fed state in 5 μl plasma collected from tail blood using an ELISA kit (Mercodia, Uppsala, Sweden).

Analysis of mRNA expression by real-time quantitative PCR

The concentration of the mRNA was determined in all experimental conditions (NC, HFD, and HFD/Ex9) during fed states in wk 4. Total RNA was isolated from the brainstem with TriPure isolation reagent (Roche Diagnostic, Meylan, France), and single-strand cDNA was synthesized from 1 μg total RNA by using oligo-deoxythymidine (RT kit; Promega, Madison, WI). Quantitative PCR was carried out with first-strand cDNA using the primers to measure UCP2, UCP3, PGC1a, PGC1b, cytochrome c (cyt c), Cox3, Cox4i, Cox7, AMPKa1, and AMPKa2 (primers available upon request at Marc.Uldry@dfci.harvard.edu) in the hind limb of mice. At wk 2, the proglucagon mRNA concentration was determined in the brainstem under the same conditions with specific primers (14).

Western blot analyses

Hind limb muscles were ground in ice-cold lysis buffer [50 mM Tris HCl (pH 7.4), with 1 mM sodium orthovanadate, 1% Triton X-100, 50 mM NaF, 0.2 mM phenylmethylsulfonyl fluoride, 100 mM NaCl, 1 mM EDTA, 1 mM EGTA, 1% Nonidet P-40], with a mixture of 0.5% protease inhibitors, sonicated and homogenized at 4 C for 2 h, and then centrifuged and the supernatant collected. Samples were analyzed by SDS-PAGE (12.5% acrylamide gel). An internal control [a mixture of total heart (50%) and adipose tissue (50%)] was also loaded. After separation, the proteins were transferred to a nitrocellulose membrane. Primary polyclonal antibody against total endothelial nitric oxide synthase (eNOS) (Santa Cruz Biotechnology, Santa Cruz, CA; dilution 1/1000), total AMP-activated kinase (AMPK) (Cell Signaling, Danvers, MA; dilution 1/1000), and actin (Cell Signaling; dilution 1/2000) as internal control were used and revealed with horseradish peroxidase-conjugated anti-rabbit IgG antibody (Amersham; dilution 1/10,000). Immunoreactivity was detected using an enhanced chemiluminescence detection kit, ECL system (Amersham, Piscataway, NJ) and exposure to x-ray film. Bands were quantified using the ImageQuant system (Amersham). UCP1 expression in BAT was measured after mitochondrial extraction. Uncoupled protein 1 (UCP1) antibody was a generous gift from Dr. D. Ricquier (Necker Hospital, Paris, France).

Weight and food intake measurements

Weight and food intake were measured weekly. The mice were housed individually. Mean daily intake was determined by averaging a 7-d total. Food spillage was considered to be 20–25% of the total amount consumed. The data were recorded three times a week over a 3-wk period because the fourth week was dedicated to different analyses and changed the feeding behavior. The weekly mean is reported. Data are presented as mean energy intake per day and per mouse.

Indirect calorimetric and ambulatory activity

Twenty-four-hour energy expenditure was measured by indirect calorimetry (Oxylet; Panlab-Bioseb, Chaville, France) between the third and the fourth week of treatment. HFD and HFD/Ex9 mice were scored for oxygen consumption (VO_2), carbon dioxide production (VCO_2), energy expenditure [calculated according to the following formula: $1.44 \times VO_2 \times (3.815 + 1.232 \times$ respiratory quotient (RQ)], and ambulatory activity. Oxygen consumption and carbon dioxide production were over a 24-h period. Ambulatory activities of the mice were monitored by an infrared photocell beam interruption method (Sedacom; Panlab-Bioseb).

Respiratory index measurement

Fresh permeabilized fibers from the extensor digitorum longus and soleus muscles were prepared to study mitochondrial respiration in cold preservation medium A [10 mM EGTA, 0.1 μM Ca, 20 mM imidazole, 20 mM taurine, 50 mM morpholinoethansulfonic acid, 0.5 mM dithiothreitol, 6.5 mM $MgCl_2$, 5.8 mM Na_2-ATP, 15 mM Na_2-phosphocreatine (pH 7.1)]. Tissues were cut into small samples and incubated at 4 C in 50 μg/ml saponin complemented medium A for 30 min under gentle agitation. Medium A was removed and replaced by a cold respiration medium B [0.5 mM EGTA, 3 mM $MgCl_2$, 60 mM K-lactobionate, 20 mM taurine, 10 mM KH_2PO_4, 20 mM HEPES, 110 mM sucrose, 1 g/liter BSA (pH 7.1)], and samples were further incubated at 4 C for 2 h under gentle agitation. Then, respiration was assessed in the Oxygraph-2k chamber (Oroboros Instruments, Innsbruck, Austria) at 30 C. State 3 of respiration was measured after addition of 20 mM glutamate, 4 mM maleate, and 10 mM ADP. State 4 of respiration was obtained after addition of 2 μg/ml oligomycin. The respiratory index was defined as the ratio between state 3 and state 4.

Body temperature measurement

Body temperature was measured in wk 4 during the fed period using a thermometer for small animals (Thermometer TK 98802; Bioseb). In another set of experiments, mice were maintained at 4 C, and the body temperature was measured every hour over 3 h in wk 4. After a 2-d recovery period, the same mice were fasted and the body temperature was measured at 6, 24, and 48 h of fasting.

TABLE 2. Plasma insulin concentrations during glucose tolerance test

Insulinemia (μU/ml)					
NC		HFD		HFD/Ex9	
−30 min	15 min	−30 min	15 min	−30 min	15 min
12.46 ± 7.72	29.74 ± 14.00	10.64 ± 6.25	41.51 ± 17.41	12.15 ± 7.90	23.37 ± 9.94

Insulin concentrations in mice fed a NC diet (n = 6) or a HFD (n = 6) and in Ex9 sc-treated mice fed a HFD (HFD/Ex9, n = 6) for 4 wk.

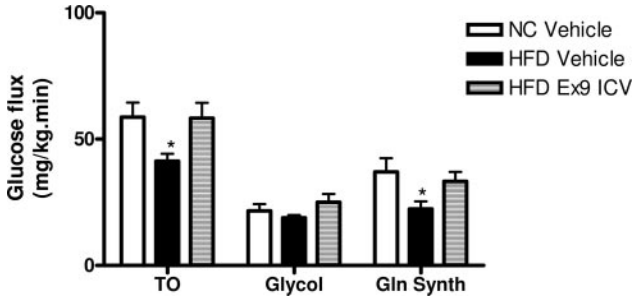

FIG. 3. Brain Ex9 reverses insulin resistance in HFD mice. Glucose flux (milligrams per kilogram per minute) was calculated in steady-state euglycemic-hyperinsulinemic conditions (5.5 mM) at a physiological insulin concentration (4 mU) in mice fed a NC diet (n = 7), or a HFD (n = 7) and in Ex9 icv-treated mice fed a HFD (HFD Ex9 ICV, n = 6) for 4 wk. Basal whole-body glucose turnover (TO), glycolysis (Glycol), and glycogen synthesis (Gln Synth) rates (milligrams per kilogram per minute) were measured. *, $P < 0.05$ *vs.* NC vehicle and HFD Ex9 icv.

Treadmill experiment

In another set of mice, endurance was analyzed by a modified procedure according to Lerman *et al.* (17). The mice were first trained to run on a simple lane treadmill (LE 8700; Bioseb) for 4 wk. Three speeds were tested for each mouse: in wk 1, 0 m/min so that the mice got used to the chamber; then in week 2, 10 m/min; and in week 3, 15 m/min. One trial was performed in wk 4 that corresponded to the experimental week. The duration of the run was recorded at each speed and was arbitrarily limited to 30 min. Three parameters were used to estimate the endurance performance: the distance (in meters) run at high speed, the number, and the time of the shocks (*i.e.* duration of electric shock given to the mice that were not running, in seconds). These last sets of data corresponded to the number of times that the mice stopped running.

Nonesterified fatty acid (NEFA) and triglyceride assays

Plasma triglycerides (Elitech Diagnostics, Salonde Provence, France) and NEFA (Wako, Richmond, VA) concentrations were measured using kits coupling enzymatic reaction and spectrophotometric detection of reaction end-products.

Calculations and statistical analyses

Results are presented as means ± SE.

The statistical significance of differences was analyzed by one-way ANOVA or two-way ANOVA (oral glucose tolerance test studies) followed by *post hoc* Bonferroni's multiple comparison test. The area under the curve was calculated using the trapezoid rule. Correlations between parameters were assessed by Pearson's correlation test, using GraphPad Prism version 4.00 for Windows (GraphPad Software, San Diego, CA; www.graphpad.com). The Student's *t* test for nonpaired values was performed in all other instances when two groups of values were compared with each other. $P < 0.05$ was regarded as statistically significant.

Results

HFD increases the expression of proglucagon mRNA in the brainstem

In a first set of experiments, we assessed whether 2 wk of a HFD affected the gut-to-brain axis before the impaired glucose metabolism classically observed after longer period such as 4 wk of high-fat feeding. We first quantified the proglucagon mRNA concentration in the brainstem. It was found to have increased by 2.5-fold when compared with NC-fed mice (Fig. 1), suggesting that an excessive GLP-1 synthesis and release might be increased in the brain during the early onset of HFD-induced metabolic diseases. After 4 wk of dietary treatment, the proglucagon mRNA concentration was increased within the same range (not shown). Interestingly, Ex9 treatment did not modify the proglucagon mRNA concentration in HFD-fed mice (Fig. 1).

Brain treatment with Ex9 ameliorates ip glucose tolerance of HFD mice

We then assessed the effect of the blockage of brain GLP-1 signaling by the means of a continuous Ex9 infusion in the brain lateral ventricle (11). Compared with NC-fed mice, HFD-fed mice exhibited a significant fasting hyperglycemia and glucose intolerance (Fig. 2A) (14). The icv treatment with Ex9 totally changed fasting glycemia and glucose tolerance to a profile similar to that observed in NC mice.

Brain Ex9 decreases fed hyperinsulinemia of HFD mice

Because we had recently shown that the activation of brain GLP-1 signaling induced hyperinsulinemia (11), we then investigated whether brain Ex9 could prevent HFD-induced hyperinsulinemia in the fed state. The continuous Ex9 treatment partially prevented fed hyperinsulinemia in HFD mice, which remained only 30% higher than the level observed in NC mice (Table 1). Importantly, in NC-fed mice, the icv Ex9 treatment has no effect on fed insulinemia and glycemia. This suggests that the diabetic state only is characterized by increased brain GLP-1 activity.

Peripheral Ex9 infusion induces glucose intolerance and reduces glucose-stimulated glycemia

To ascertain that the improved glucose tolerance and reduced hyperinsulinemia observed when Ex9 was infused into the brain was specific to the central and not to a systemic action

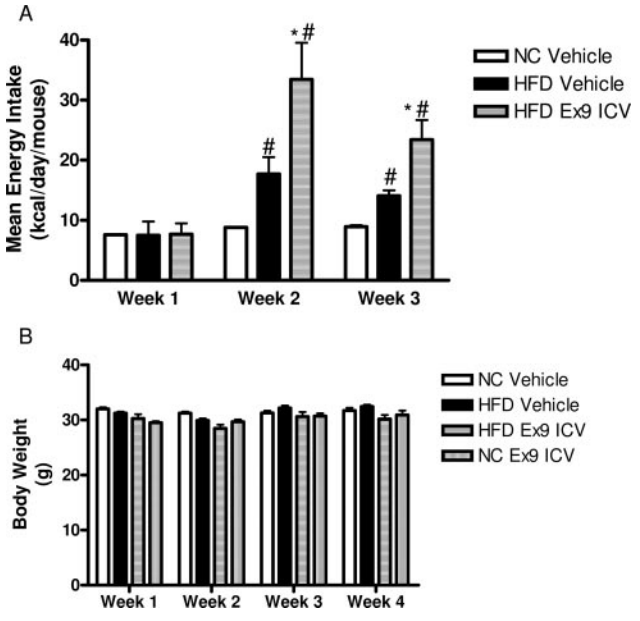

FIG. 4. Brain Ex9 increases energy intake without affecting body weight. A, Mean energy intake (kilocalories per day per mouse) for 3 wk. *, $P < 0.05$ *vs.* NC vehicle and HFD vehicle; #, $P < 0.05$ *vs.* NC vehicle; B, weekly body weight (grams) of mice fed a NC (n = 6) and in Ex9 icv-treated mice fed a NC diet or a -HFD (n = 6) and in Ex9 icv-treated mice fed a HFD (HFD Ex9 ICV, n = 7) for 4 wk.

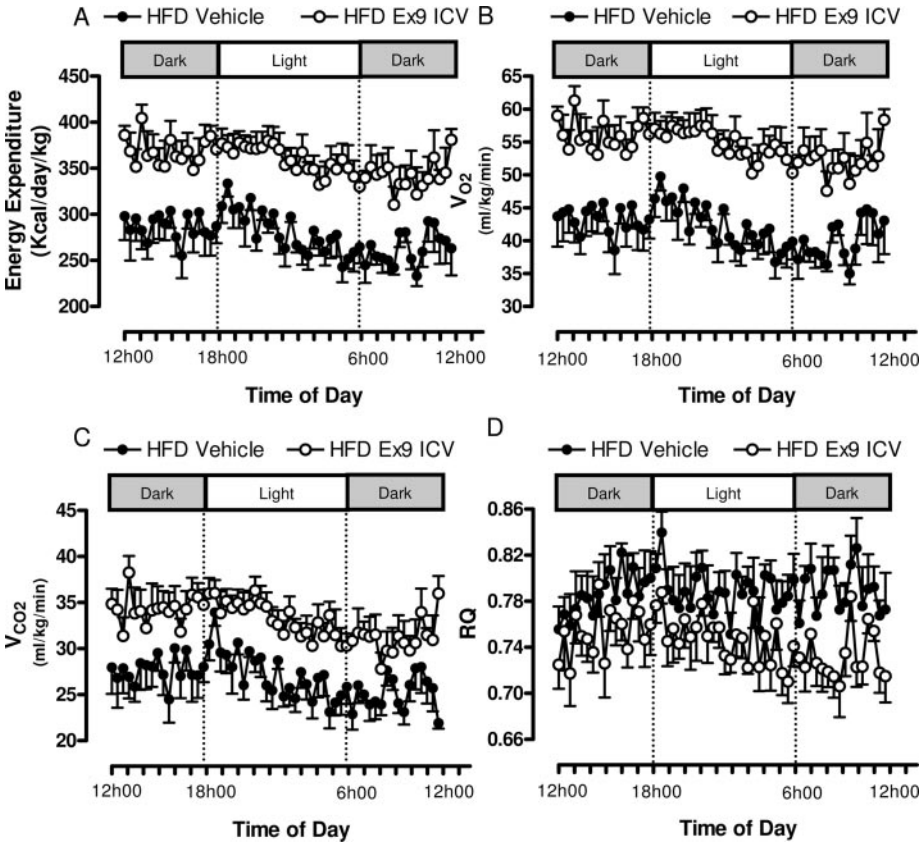

FIG. 5. Brain Ex9 increases energy expenditure, oxygen consumption, carbon dioxide production, insulin-dependent muscle glucose utilization, and respiratory index. A, Energy expenditure (kilocalories per day per kilogram); B, oxygen consumption ($V_{O2,}$ milliliters per kilogram per minute) C, carbon dioxide production ($V_{CO2,}$ milliliters per kilogram per minute); D, respiratory quotient (RQ) in mice fed a HFD (HFD Vehicle, n = 7) and in Ex9 icv-treated mice fed a HFD (HFD Ex9 icv, n = 7) for 4 wk. This increase in metabolic rate was associated with an augmentation of the glucose utilization rate only in insulin-sensitive muscle, as measured *in vivo* by means of the 2DG tracer technique (E and F). Individual tissue glucose utilization rates (nanograms per milligram per minute) were assessed during the clamp studies in adipose depots (WAT and BAT), in muscles [vastus lateralis (VL)], and heart in mice fed a NC diet (NC Vehicle, n = 6), or a HFD (HFD Vehicle, n = 10) and in Ex9 icv-treated mice fed a HFD (HFD Ex9 ICV, n = 8) for 4 wk. *, $P < 0.05$ *vs.* NC vehicle; #, $P < 0.05$ *vs.* NC vehicle and HFD vehicle Ex9; §, $P < 0.05$ *vs.* NC vehicle and HFD vehicle. G, Respiratory index of mitochondrial respiration in freshly permeabilized muscle fibers of mice fed a NC diet (NC Vehicle, n = 5), or a HFD (HFD Vehicle, n = 5) and in Ex9 icv-treated mice fed a HFD (HFD Ex9 ICV, n = 5) for 4 wk. #, $P < 0.05$ *vs.* NC vehicle and HFD Ex9 icv.

of GLP-1, we infused one set of HFD-fed mice with Ex9 sc for 1 month. The data show that the glucose tolerance and fasted glycemia were worsened by the systemic infusion of Ex9 (Fig. 2B). This effect was opposite to that observed when Ex9 was infused into the brain (Fig. 2A), demonstrating that the central Ex9 infusion was restricted to the brain and had no systemic consequences. Furthermore, glucose-induced hyperinsulinemia in the HFD mice was normalized by the Ex9 treatment (Table 2).

Brain Ex9 reverses insulin resistance in HFD mice

Together with glucose intolerance and fed hyperinsulinemia, insulin resistance is another feature of the onset of diabetes. To assess whether the brain Ex9 treatment of the HFD mice was associated with changes in insulin sensitivity, we performed a euglycemic-hyperinsulinemic clamp at a physiological insulin concentration (4 mU) and measured glucose flux. HFD mice were insulin resistant (15) (Fig. 3) with a significant decrease in glycogen synthesis rather than glycolysis, as described for type 2 diabetes (18, 19). Again, Ex9 treatment restored insulin sensitivity in HFD mice to meet values of NC mice.

Brain Ex9 increases energy intake without any effect on body weight

Here we confirmed that increased energy intake is another major feature of the onset of HFD-induced diabetes (Fig. 4A) when compared with NC mice (14, 20). The Ex9 treatment further increased the mean energy intake (Fig. 4A) when compared with HFD-vehicle and NC mice. However, body weight did not increase accordingly (Fig. 4B). Both observations could be reconciled by suggesting that mechanisms of energy expenditure have been triggered.

Brain Ex9 increases energy expenditure, oxygen consumption, carbon dioxide production, and insulin-dependent glucose utilization by muscle

We then assessed the energy expenditure by indirect calorimetric methods. The data showed that Ex9 treatment increased energy expenditure, oxygen consumption, and carbon dioxide production in the HFD diabetic mice (Fig. 5, A–C). This was associated with a reduction of the respiratory quotient (RQ) that became close to 0.75 (Fig. 5D) and corresponds to increased lipid oxidation. This increase in metabolic rate was associated with increased insulin-sensitive glucose utilization by muscle (vastus lateralis and heart) as assessed *in vivo* by the D-[^{3}H]2DG tracer technique (Fig. 5, E and F). In addition, D-[^{3}H]2DG utilization by the WAT and the BAT was reduced by the HFD treatment (Fig. 5F). It was partially reversed by Ex9 in the WAT only (Fig. 5F). Importantly, icv Ex9 treatment corrected the impaired respiratory index observed in glycolytic (extensor digitorum longus, which are the most representative muscle fiber types of the body) but not oxidative muscles (soleus) (Fig. 5G).

Brain Ex9 increases skeletal muscle eNOS and UCP2 expression

To elaborate some of the molecular events that could be responsible for the increased metabolism in glycolytic

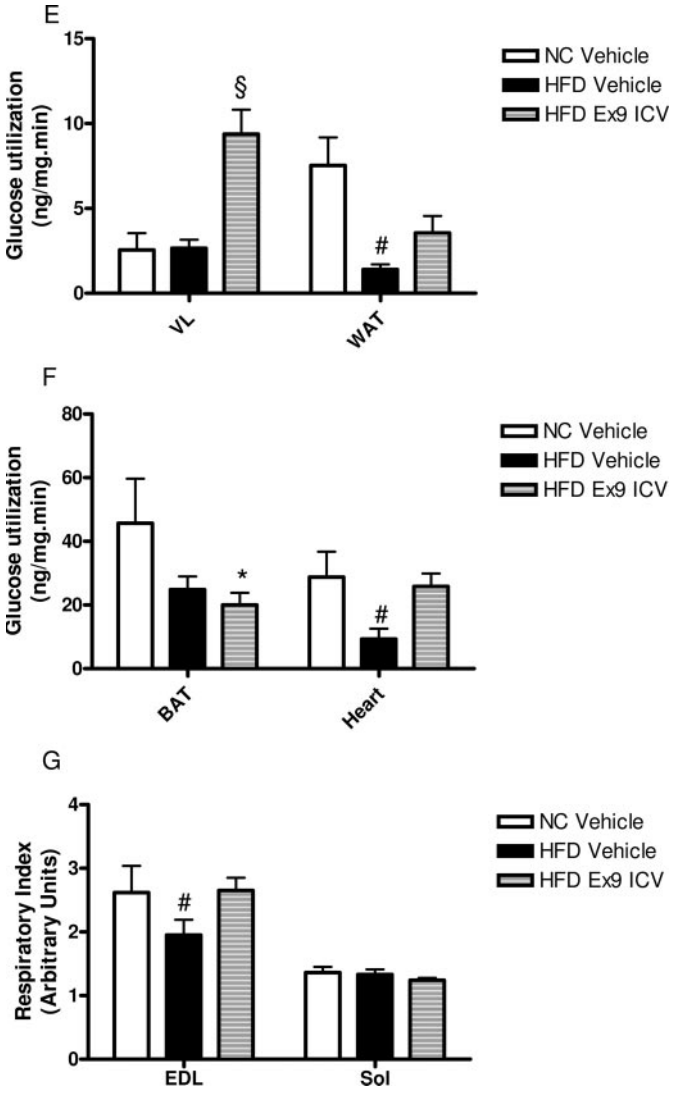

FIG. 5. *Continued*

skeletal muscle induced by Ex9 treatment, we measured AMPK expression. No significant differences were observed (Fig. 6A). As opposed to AMPK, eNOS expression was doubled in the Ex9-treated mice when compared with the other groups (Fig. 6B). Because the respiratory index was increased by the Ex9 treatment, we next assessed genes involved in mitochondrial metabolism and showed that the relative mRNA concentrations of UCP2 was increased (Fig. 6C). This change could be attributed to differences in the plasma NEFA concentrations because they correlated positively with UCP2 mRNA levels (21, 22) (Fig. 6, D–G). Interestingly, UCP3 mRNA concentration was increased during high-fat feeding, but Ex9 treatment had no further effect. We also analyzed a large set of mRNA encoding mitochondrial proteins. No differences were observed between the experimental groups (Fig. 6H).

Brain Ex9 increases ambulatory activity without increasing endurance during physical exercise

Because the above data showed that the blocking of brain GLP-1 signaling increased energy expenditure and the respiratory index of glycolytic muscle, we investigated whether this impacted on ambulatory activity as a means of increasing energy expenditure. The data showed that icv Ex9 treatment increased the ambulatory activity (Fig. 7A), and so we next assessed whether endurance during exercise was also affected as another way of increasing energy expenditure. The data showed that icv Ex9 did not affect the total distance run by the mice or the number and the duration of the shocks (Fig. 7, B–D).

Brain Ex9 controls body temperature and glycemia in response to cold exposure-induced feeding but not in response to fasting

Another mechanism through which energy expenditure could be increased is metabolic thermogenesis. First, in response to cold exposure-induced feeding, rectal body temperature decreased similarly in all experimental groups. Body temperature was lower in the HFD than in the NC group when the mice were kept at +4 C for at least 180 min. The body temperature was normalized in the icv Ex9-treated group (Fig. 8A). As a result of cold exposure-induced feeding, glycemia increased in NC-fed mice but not in the HFD and HFD/Ex9 mice after 60 min (Fig. 8B). Conversely, HFD/Ex9 mice had significantly increased glycemia after 120 and 180 min compared with HFD-fed mice (Fig. 8B). Interestingly, the UCP1 concentration was unchanged, supporting the idea that an increased whole-body metabolism rather than adaptive BAT-dependent thermogenesis was involved (Fig. 8C). In response to fasting, the rectal body temperature decreased similarly in all experimental groups (Fig. 8D).

Discussion

High-fat feeding induces hyperinsulinemia and insulin resistance, two major features of type 2 diabetes. We have shown in this study that at the onset of diabetes, the blockage of brain GLP-1 signaling prevents both characteristics. A further observation was that Ex9 infusion into the brain increased energy intake without a gain in body weight. The mechanism of such paradoxical effects was that the blockage of brain GLP-1 receptor signaling increased energy expenditure through a mechanism involving absorptive but not fasting thermogenesis. Altogether, our data showed that in response to high-fat feeding, an excessive brain GLP-1 signaling contributes to hyperinsulinemia, insulin resistance, and energy storage.

Over the last decade, the peripheral tissue-to-brain axis has been considered as a major regulator for the control of blood glucose homeostasis, notably through the central role of insulin and leptin (10). More recently, gut hormones like the incretins or ghrelin have been shown to regulate energy metabolism through interactions with brain nuclei (11, 23, 24). We previously showed that brain GLP-1 signaling increased glucose-stimulated insulin secretion (11). Therefore, we hypothesized that excessive stimulation of the gut-to-brain axis, such as during high calorie intake, could mediate overt brain GLP-1 signaling leading to hyperinsulinemia. We used an animal model of diabetes induced by a fat-enriched diet. To overcome the effect of obesity on the occurrence of diabetes, we eliminated carbohydrate from the diet. This

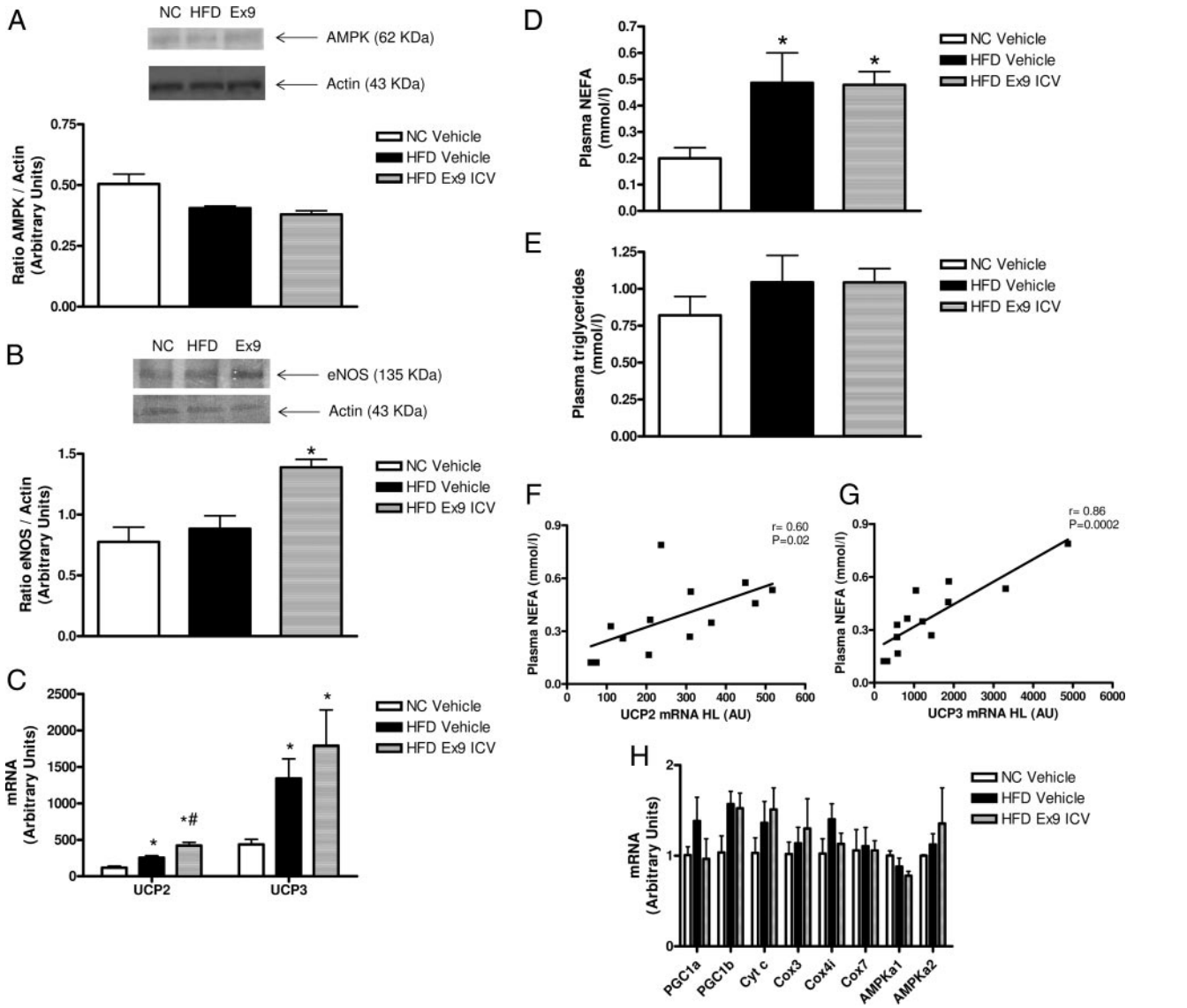

FIG. 6. Brain Ex9 increases eNOS and UCP2 expression in glycolytic muscles and raises plasma NEFA and triglyceride concentrations. A and B, Representative Western blot analysis and quantification of AMPK (A) and eNOS (B) expression in skeletal muscles. Given the increase in the respiratory index, we next assessed genes involved in mitochondrial metabolism. C, UCP2 and UCP3 mRNA concentrations in muscles (arbitrary units); D, plasma NEFA (millimoles per liter); E, plasma triglycerides (millimoles per liter); F and G, Pearson's correlation between muscles' UCP2 mRNA and plasma NEFA (F) and UCP3 mRNA and plasma NEFA (G) concentrations (Pearson r and *P* value appears as *inset* in the graphs); H, mRNA concentrations encoding mitochondrial proteins in mice fed a NC diet (NC Vehicle, n = 5), or a HFD (HFD Vehicle, n = 6) and in Ex9 icv-treated mice fed a HFD (HFD Ex9 icv, n = 6) for 4 wk. *, $P < 0.05$ *vs.* NC Vehicle; #, $P < 0.05$ *vs.* HFD vehicle.

induces diabetes and insulin resistance before overt obesity, as has been described (12). First, our present data show that mice fed a HFD were characterized by a 3-fold increase in proglucagon mRNA in the brainstem. This brain structure expresses the proglucagon gene (25, 26), whereas the GLP-1 receptor is present in hypothalamic nuclei as shown by *in situ* hybridization (27), binding experiments (28, 29), or autoradiography (30). Interestingly, the GLP-1 receptor mRNA was also colocalized with other molecular factors involved in the brain glucose sensor mechanism, such as the glucose transporter GLUT2 and the glucokinase gene (31, 32). Our second set of data showed that at the onset of HFD-induced diabetes, a sustained brain GLP-1 signaling is required for the maintenance of fed hyperinsulinemia. The continuous blockage of brain GLP-1 signaling efficiently prevented HFD-induced fed hyperinsulinemia and consequently insulin resistance. The improved insulin sensitivity was associated with an increased rate of glycogen synthesis, because it is an important characteristic of muscle insulin resistance (33–35). High-fat feeding is characterized by increased intestinal proglucagon gene expression and GLP-1 production (15). Because GLP-1 readily diffuses across the blood-brain barrier, it cannot be ruled out that systemic GLP-1 could be responsible for the activation of brain GLP-1 signaling. To eliminate this hypothesis, we infused HFD-fed mice for 4 wk with Ex9 sc. Under such conditions, glucose intolerance was worsened. Because this observation was opposite to that obtained using the brain GLP-1 receptor blockage procedure, we can rule out

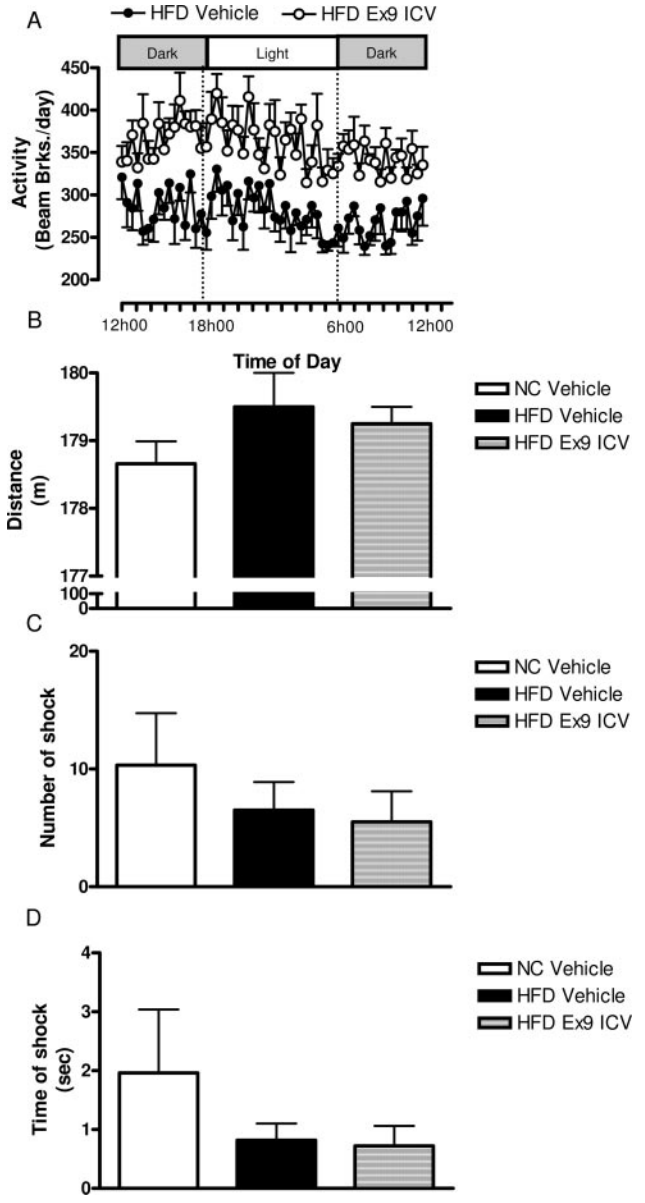

FIG. 7. Brain Ex9 increases ambulatory activity without increasing endurance during physical exercise. A, Ambulatory activity (Beam Brks./day) in mice fed a NC diet (NC Vehicle, n = 6), or a HFD (HFD Vehicle, n = 7) and in Ex9 icv-treated mice fed a HFD (HFD Ex9 ICV, n = 7) for 4 wk; B–D, treadmill endurance during physical exercise: running distance (meters) (B), number of shocks (electric shock given to the mice when not running) (C), and time of shocks (seconds) (D) in mice fed a NC diet (NC Vehicle, n = 5), or a HFD (HFD Vehicle, n = 4) and in Ex9 icv-treated mice fed a HFD (HFD Ex9 ICV, n = 4) for 4 wk.

a direct systemic effect of central GLP-1 on the control of glucose metabolism.

The molecular mechanisms responsible for brain GLP-1-induced insulin resistance are unknown but could be related to changes in muscle AMPK (36, 37) and eNOS activities (38, 39). Our data showed that the brain Ex9 treatment almost doubled the eNOS concentration in the skeletal muscle without, however, changes in AMPK gene expression. We and others previously showed the importance of eNOS for the control of insulin resistance by the euglycemic-hyperinsulinemic clamp in corresponding knockout mice (39, 40, 41, 42) (43). Similarly, the molecular mechanisms in the brain that relate to the transmission of the GLP-1 signal toward peripheral tissues are unknown. In a subset of experiments, minor increases of proopiomelanocortin and NPY mRNA concentrations were detected in the brain of HFD/Ex9-treated mice (data not shown). The interpretation of such changes is not yet clear and remains to be further analyzed.

Metabolic diseases are associated with increased energy intake, and it has been previously reported that brain GLP-1 reduces food intake (44–46). Our data showed that HFD-fed mice simultaneously infused with Ex9 into the brain exhibited increased energy intake. However, this was not accompanied by a concomitant increase in body weight. To understand this paradoxical observation, we quantified the energy expenditure and showed that the blockage of brain GLP-1 signaling dramatically increased carbon dioxide production and oxygen consumption. This was associated with increased insulin-stimulated glucose utilization in skeletal muscle. As a consequence, whole-body energy expenditure was stimulated by the icv Ex9 treatment of the diabetic mice. A recent report showed that systemic GLP-1 controlled energy expenditure. GLP-1 receptor$^{-/-}$ and the double incretin receptor knockout (DIRKO) mice also exhibited increased energy expenditure on NC as well as when fed a HFD during both light and dark phases of the feeding cycle. Furthermore, DIRKO mice exhibited resistance to diet-induced obesity. Remarkably, although DIRKO mice also exhibited increased food intake, the dominant effect of increased energy expenditure resulted in a failure to gain weight on both a NC diet and a HFD. Similar to our results, the data from Hansotia *et al.* (3) revealed that the increased energy expenditure, in both single incretin receptor knockout and DIRKO mice, is attributable, at least in part, to increased locomotor activity. These observations suggest that the importance of GLP-1 action, as a negative regulator of energy intake, is balanced by the role of GLP-1 in the control of locomotor activity (47). This resulted in resistance to diet-induced obesity despite increased energy intake in GLP-1 receptor$^{-/-}$ and DIRKO mice (3). However, in that previous study, the extrapancreatic tissues responsible for this phenotype were unknown. We have shown in this current study that brain GLP-1 was responsible for the regulation of energy storage because the blockage of brain GLP-1 signaling during HFD-induced diabetes increased energy expenditure. The increased energy expenditure was associated with an increased ambulatory capacity. In addition, our data show that cold exposure-induced feeding decreased body temperature in all experimental conditions, but more drastically in HFD mice. This phenotype was reversed by icv Ex9 treatment and associated with an increased expression of UCP2 in skeletal muscle.

Altogether, our data demonstrate that the onset of HFD-induced diabetes is associated with an increased brain GLP-1 signaling associated with hyperinsulinemia, insulin resistance, and energy storage. This study demonstrates the importance of extrapancreatic functions controlled by brain GLP-1, which together lead to increased energy storage as would be logical for a hormone secreted in the absorptive state.

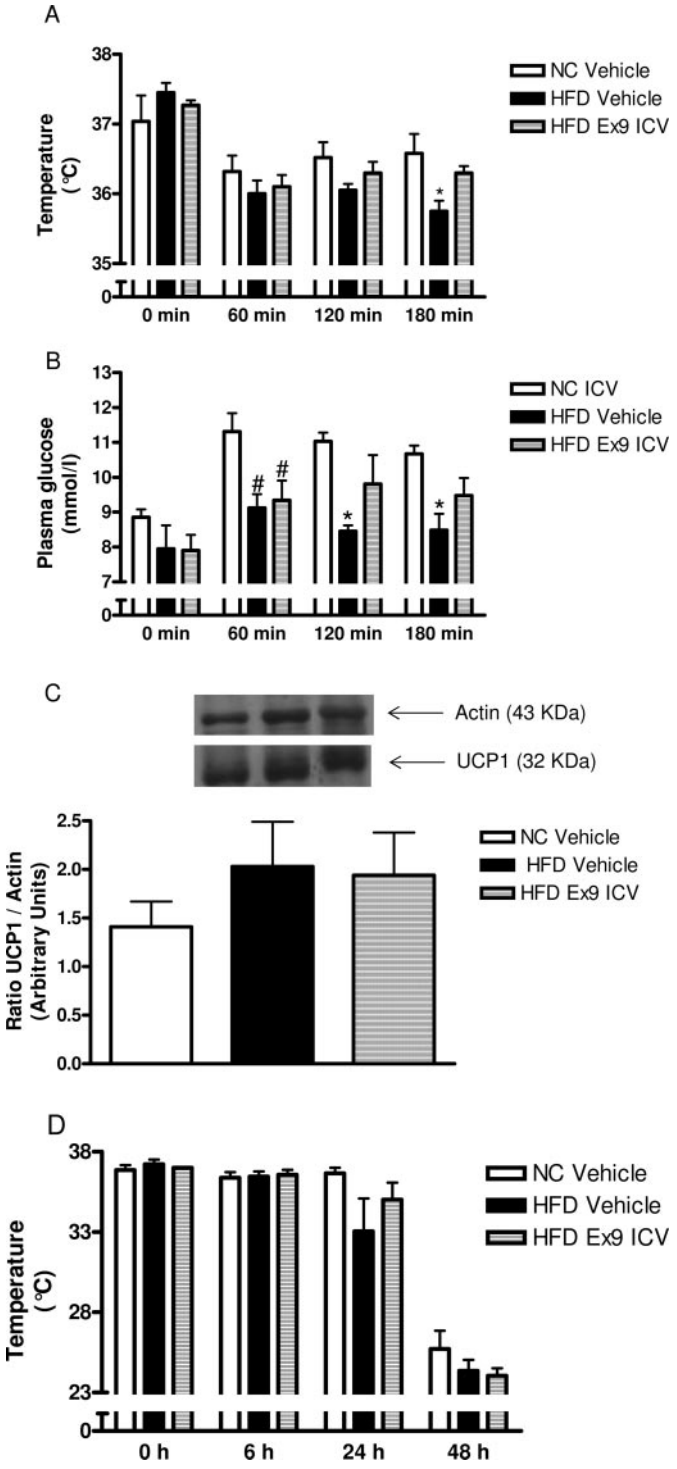

FIG. 8. Brain Ex9 controls body temperature and glycemia in response to cold-induced feeding but not in response to fasting. A and B, Metabolic parameters during cold exposure for up to 180 min: body temperature (°C) (A) and plasma glucose (millimoles per liter) (B); C, representative Western blot analysis and quantification of UCP1 in mitochondria extracted from BAT; D, body temperature after 6, 24, and 48 h of fasting in mice fed a NC diet (NC Vehicle, n = 5), or a HFD (HFD Vehicle, n = 4) and in Ex9 icv-treated mice fed a HFD (HFD Ex9 ICV, n = 4) for 4 wk. *, $P < 0.05$ *vs.* NC vehicle and HFD Ex9 icv; #, $P < 0.05$ *vs.* NC vehicle.

Acknowledgments

We thank Prof. Louis Casteilla for helpful discussion. R.B., C.K., and P.D.C. are members of CESNA (Club d'Etude du Système Nerveux Autonome) and are grateful for its financial support. We fully acknowledge the expertise of Laurent Montbrun and Sophie Le Gonidec from the functional exploration platform, Toulouse-Midi-Pyrenees-Genopole concerning energy expenditure measurements, and Danièle Daviaud for technical advice. We also thank Dr. John Woodley for editing the English.

Received February 7, 2008. Accepted June 5, 2008.

Address all correspondence and requests for reprints to: Institut de Medecine Moleculaire de Rangueil (I2MR), Institut National de la Santé et de la Recherche Médicale Unité 858, Institut Fédératif de Recherche 31, Centre Hospitalier Universitaire Rangueil, BP84225, 31432 Toulouse Cedex 4, France. E-mail: remy.burcelin@inserm.fr.

R.B. and C.K. were supported in part by operating grants from Merck Sharp & Dohme Chibret, ALFEDIAM/NOVARTIS, EFSD-Amylin (ANR, program Aliment Santé:Nutrisens, Mithycal, Metaprofile, and program Physiopathologie: brain GLP-1), and from l'Association pour la Recherche sur le Diabète in the context of the Programe National de Recherche sur le Diabète (PNRD). P.D.C. was supported in part by grants from the Fonds de la Recherche Scientifique and Fond pour la recherche scientifique (FRS) from the Université Catholique de Louvain. P.D.C. is Postdoctoral Researcher from the Fonds de la Recherche Scientifique (Brussels, Belgium).

R.B. analyzed the data; C.K., P.D.C., and R.B. wrote the paper.

Disclosure Statement: The authors declare that they have no conflict of interest.

References

1. **Drucker DJ** 1990 Glucagon and the glucagon-like peptides. Pancreas 5:484–488
2. **Nauck M** 1996 Therapeutic potential of glucagon-like peptide 1 in type 2 diabetes. Diabetic Medicine 13:S39–S43
3. **Hansotia T, Maida A, Flock G, Yamada Y, Tsukiyama K, Seino Y, Drucker DJ** 2007 Extrapancreatic incretin receptors modulate glucose homeostasis, body weight, and energy expenditure. J Clin Invest 117:143–152
4. **Burcelin R, Da Costa A, Drucker D, Thorens B** 2001 Glucose competence of the hepatoportal vein sensor requires the presence of an activated glucagon-like peptide-1 receptor. Diabetes 50:1720–1728
5. **Burcelin R, Dolci W, Thorens B** 2000 Glucose sensing by the hepatoportal sensor is GLUT-2 dependent. In vivo analysis in GLUT-2-null mice. Diabetes 49
6. **Thorens B** 1996 Glucose transporters in the regulation of intestinal, renal, and liver glucose fluxes. Am J Physiol 270:G541–G553
7. **Burcelin R, Dolci W, Thorens B** 2000 Portal glucose infusion in the mouse induces hypoglycemia. Evidence that the hepatoportal glucose sensor stimulates glucose utilization. Diabetes 49:1635–1642
8. **Moore MC, Cherrington AD** 1996 The nerves, the liver, and the route of feeding: an integrated response to nutrient delivery. Nutrition 12:282–284
9. **Hevener AL, Bergman RN, Donovan CM** 1997 Novel glucosensor for hypoglycemic detection localized to the portal vein. Diabetes 46:1521–1525
10. **Obici S, Feng Z, Arduini A, Conti R, Rossetti L** 2003 Inhibition of hypothalamic carnitine palmitoyltransferase-1 decreases food intake and glucose production. Nat Med 9:756–761
11. **Knauf C, Cani P, Perrin C, Iglesias M, Maury J, Bernard E, Benhamed F, Grémeaux T, Drucker D, Kahn C, Girard J, Tanti J, Delzenne N, Postic C, Burcelin R** 2005 Brain glucagon-like peptide-1 increases insulin secretion and muscle insulin resistance to favor hepatic glycogen storage. J Clin Invest 115:3554–3563
12. **Burcelin R, Crivelli V, Dacosta A, Roy-Tirelli A, Thorens B** 2002 Heterogeneous metabolic adaptation of C57BL/6J mice to high-fat diet. Am J Physiol Endocrinol Metab 282:E834–E842
13. **Perrin C, Knauf C, Burcelin R** 2004 Intracerebroventricular infusion of glucose, insulin, and the adenosine monophosphate-activated kinase activator, 5-aminoimidazole-4-carboxamide-1-β-D-ribofuranoside, controls muscle glycogen synthesis. Endocrinology 145:4025–4033
14. **Cani P, Amar J, Iglesias M, Poggi M, Knauf C, Bastelica D, Neyrinck A, Fava F, Tuohy K, Chabo C, Waget A, Delmée E, Cousin B, Sulpice T, Chamontin B, Ferrières J, Tanti J, Gibson G, Casteilla L, Delzenne N, Alessi M, Burcelin R** 2007 Metabolic endotoxemia initiates obesity and insulin resistance. Diabetes 56:1761–1772
15. **Cani PD, Knauf C, Iglesias M, Drucker D, Delzenne N, Burcelin R** 2006 Improvement of glucose tolerance and hepatic insulin sensitivity by oligofructose requires a functional GLP-1 receptor. Diabetes 55:1484–1490
16. **Knauf C, Rieusset J, Foretz M, Cani PD, Uldry M, Hosokawa M, Martinez E, Bringart M, Waget A, Kersten S, Desvergne B, Gremlich S, Wahli W,**

Seydoux J, Delzenne NM, Thorens B, Burcelin R 2006 Peroxisome proliferator-activated receptor-α-null mice have increased white adipose tissue glucose utilization, GLUT4, and fat mass: role in liver and brain. Endocrinology 147:4067–4078

17. **Lerman I, Harrison BC, Freeman K, Hewett TE, Allen DL, Robbins J, Leinwand LA** 2002 Genetic variability in forced and voluntary endurance exercise performance in seven inbred mouse strains. J Appl Physiol 92:2245–2255
18. **Newgard CB, Brady MJ, O'Doherty RM, Saltiel AR** 2000 Organizing glucose disposal: emerging roles of the glycogen targeting subunits of protein phosphatase-1. Diabetes 49:1967–1977
19. **Solini A, Di Virgilio F, Chiozzi P, Fioretto P, Passaro A, Fellin R** 2001 A defect in glycogen synthesis characterizes insulin resistance in hypertensive patients with type 2 diabetes. Hypertension 37:1492–1496
20. **Cani PD, Neyrinck AM, Fava F, Knauf C, Burcelin RG, Tuohy KM, Gibson GR, Delzenne NM** 2007 Selective increases of bifidobacteria in gut microflora improve high-fat-diet-induced diabetes in mice through a mechanism associated with endotoxaemia. Diabetologia 50:2374–2383
21. **Murray AJ, Panagia M, Hauton D, Gibbons GF, Clarke K** 2005 Plasma free fatty acids and peroxisome proliferator-activated receptor α in the control of myocardial uncoupling protein levels. Diabetes 54:3496–3502
22. **Petzke KJ, Friedrich M, Metges CC, Klaus S** 2005 Long-term dietary high protein intake up-regulates tissue specific gene expression of uncoupling proteins 1 and 2 in rats. Eur J Nutr 44:414–421
23. **Drucker DJ** 2007 The role of gut hormones in glucose homeostasis. J Clin Invest 117:24–32
24. **D'Alessio DA, Sandoval DA, Seeley RJ** 2005 New ways in which GLP-1 can regulate glucose homeostasis. J Clin Invest 115:3406–3408
25. **Blazquez E, Alvarez E, Navarro M, Roncero I, Rodriguez-Fonseca F, Chowen JA, Zueco JA** 1998 Glucagon-like peptide-1(7–36) amide as a novel neuropeptide. Mol Neurobiol 18:157–173
26. **Alvarez E, Martinez MD, Roncero I, Chowen JA, Garcia-Cuartero B, Gispert JD, Sanz C, Vazquez P, Maldonado A, de Caceres J, Desco M, Pozo MA, Blazquez E** 2005 The expression of GLP-1 receptor mRNA and protein allows the effect of GLP-1 on glucose metabolism in the human hypothalamus and brainstem. J Neurochem 92:798–806
27. **Navarro M, Rodriquez de Fonseca F, Alvarez E, Chowen JA, Zueco JA, Gomez R, Eng J, Blazquez E** 1996 Colocalization of glucagon-like peptide-1 (GLP-1) receptors, glucose transporter GLUT-2, and glucokinase mRNAs in rat hypothalamic cells: evidence for a role of GLP-1 receptor agonists as an inhibitory signal for food and water intake. J Neurochem 67:1982–1991
28. **Goke R, Larsen PJ, Mikkelsen JD, Sheikh SP** 1995 Identification of specific binding sites for glucagon-like peptide-1 on the posterior lobe of the rat pituitary. Neuroendocrinology 62:130–134
29. **Goke R, Larsen PJ, Mikkelsen JD, Sheikh SP** 1995 Distribution of GLP-1 binding sites in the rat brain: evidence that exendin-4 is a ligand of brain GLP-1 binding sites. Eur J Neurosci 7:2294–2300
30. **Uttenthal LO, Toledano A, Blazquez E** 1992 Autoradiographic localization of receptors for glucagon-like peptide-1 (7–36) amide in rat brain. Neuropeptides 21:143–146
31. **Matschinsky FM** 1996 A lesson in metabolic regulation inspired by the glucokinase paradigm. Diabetes 45:223–241
32. **Marty N, Dallaporta M, Foretz M, Emery M, Tarussio D, Bady I, Binnert C, Beermann F, Thorens B** 2005 Regulation of glucagon secretion by glucose transporter type 2 (glut2) and astrocyte-dependent glucose sensors. J Clin Invest 115:3545–3553
33. **Frontoni S, Choi SB, Banduch D, Rossetti L** 1991 In vivo insulin resistance induced by amylin primarily through inhibition of insulin-stimulated glycogen synthesis in skeletal muscle. Diabetes 40:568–573
34. **Rossetti L, Giaccari A** 1990 Relative contribution of glycogen synthesis and glycolysis to insulin-mediated glucose uptake. A dose-response euglycemic clamp study in normal and diabetic rats. J Clin Invest 85:1785–1792
35. **Shulman GI, Rothman DL, Jue T, Stein P, DeFronzo RA, Shulman RG** 1990 Quantitation of muscle glycogen synthesis in normal subjects and subjects with non-insulin-dependent diabetes by ^{13}C nuclear magnetic resonance spectroscopy. N Engl J Med 322:223–228
36. **Viollet B, Andreelli F, Jorgensen SB, Perrin C, Flamez D, Mu J, Wojtaszewski JF, Schuit FC, Birnbaum M, Richter E, Burcelin R, Vaulont S** 2003 Physiological role of AMP-activated protein kinase (AMPK): insights from knockout mouse models. Biochem Soc Trans 31:216–219
37. **Viollet B, Andreelli F, Jorgensen SB, Perrin C, Geloen A, Flamez D, Mu J, Lenzner C, Baud O, Bennoun M, Gomas E, Nicolas G, Wojtaszewski JF, Kahn A, Carling D, Schuit FC, Birnbaum MJ, Richter EA, Burcelin R, Vaulont S** 2003 The AMP-activated protein kinase α2 catalytic subunit controls whole-body insulin sensitivity. J Clin Invest 111:91–98
38. **Shankar R, Zhu J, Ladd B, Henry D, Shen H, Baron A** 1998 Central nervous system nitric oxide synthase activity regulates insulin secretion and insulin action. J Clin Invest 102:1403–1412
39. **Duplain H, Burcelin R, Sartori C, Cook S, Egli M, Lepori M, Vollenweider P, Pedrazzini T, Nicod P, Thorens B, Scherrer U** 2001 Insulin resistance, hyperlipidemia and hypertension in mice lacking endothelial nitric oxide synthase. Circulation 104:342–345
40. **Shankar RR, Wu Y, Shen HQ, Zhu JS, Baron AD** 2000 Mice with gene disruption of both endothelial and neuronal nitric oxide synthase exhibit insulin resistance. Diabetes 49:684–687
41. **Cook S, Hugli O, Egli M, Vollenweider P, Burcelin R, Nicod P, Thorens B, Scherrer U** 2003 Clustering of cardiovascular risk factors mimicking the human metabolic syndrome X in eNOS null mice. Swiss Med Wkly 133:360–363
42. **Cook S, Hugli O, Egli M, Menard B, Thalmann S, Sartori C, Perrin C, Nicod P, Thorens B, Vollenweider P, Scherrer U, Burcelin R** 2004 Partial gene deletion of endothelial nitric oxide synthase predisposes to exaggerated high-fat diet-induced insulin resistance and arterial hypertension. Diabetes 53:2067–2072
43. **Cabou C, Cani PD, Campistron G, Knauf C, Mathieu C, Sartori C, Amar J, Scherrer U, Burcelin R** 2007 Central insulin regulates heart rate and arterial blood flow: an endothelial nitric oxide synthase-dependent mechanism altered during diabetes. Diabetes 56:2872–2877
44. **Furuse M, Matsumoto M, Okumura J, Sugahara K, Hasegawa S** 1997 Intracerebroventricular injection of mammalian and chicken glucagon-like peptide-1 inhibits food intake of the neonatal chick. Brain Res 755:167–169
45. **Thiele TE, Van Dijk G, Campfield LA, Smith FJ, Burn P, Woods SC, Bernstein IL, Seeley RJ** 1997 Central infusion of GLP-1, but not leptin, produces conditioned taste aversions in rats. Am J Physiol 272:R726–R730
46. **Tang-Christensen M, Larsen PJ, Goke R, Fink-Jensen A, Jessop DS, Moller M, Sheikh SP** 1996 Central administration of GLP-1-(7–36) amide inhibits food and water intake in rats. Am J Physiol 271:R848–R856
47. **Ayala JE, Bracy DP, Hansotia T, Flock G, Seino Y, Wasserman DH, Drucker DJ** 2008 Insulin action in the double incretin receptor knockout mouse. Diabetes 57:288–297

***Endocrinology* is published monthly by The Endocrine Society (http://www.endo-society.org), the foremost professional society serving the endocrine community.**